ACCEPTED MANUSCRIPT
Review of Scientific Instruments
AIP Publishing
This is the author's peer reviewed, accepted manuscript. However, the online version of record will be different from this version once it has been copyedited and typeset.
PLEASE CITE THIS ARTICLE AS DOI:10.1063/5.0101550

Faraday-effect polarimetry for current profile measurement in the tokamak plasma edge

J. Chen[a)], D. L. Brower and T. Benedett

University of California Los Angeles, Los Angeles, California 90095, USA

Toroidal current profile measurements in the tokamak plasma edge are critical for fusion plasma physics research and model validation. A three-wave Faraday-effect polarimeter-interferometer with a sub-centimeter spatial resolution is proposed on the DIII-D tokamak to determine edge current profile via Abel inversion. Using probe beams with 316 μm wavelength, a low-field-side, vertical-view, single-pass optical layout covering the plasma edge region (R=2.15-2.27 m) is assessed. Measurements with no greater than 0.1 degree polarimetric systematic uncertainty, no greater than 0.01 degree polarimetric root-mean-square (RMS) noise (1 kHz bandwidth) and a 0.8 cm radial chord spacing is considered feasible, based on the achieved performance of existing systems using similar wavelengths on fusion devices. Synthetic diagnostic calculations taking various factors into account, such as diagnostic uncertainty and quality of magnetic flux surfaces, find that the edge current profile can be determined with up to 0.12 MA/m^2 uncertainty, or about 10% of the peak current density in the pedestal of an investigated high-confinement plasma.

I. INTRODUCTION

Measuring the plasma current profile in the tokamak plasma edge, especially in the pedestal region of high-confinement (H-) mode plasmas, is of great interest for understanding physics, such as the H-mode pedestal formation[1] , and for validating models, such as the bootstrap current model[2]. H-mode pedestal plasmas have a steep current gradient with narrow width, making the current profile measurement extremely challenging. Optical polarimetry measures the line-integrated, electron density-weighted magnetic field in high-temperature magnetized plasmas via the Faraday-effect, $\alpha = 2.62 \times 10^{-13}\lambda^2 \int n_e B_l dl$, where α is the Faraday rotation angle, λ is the probe beam wavelength, n_e is the plasma electron density, l is the probe beam trajectory and B_l is the magnetic field component along l. Interferometry can be combined with polarimetry to simultaneously detect the line-integrated electron density along the same optical path, $\varphi = 2.82 \times 10^{-15}\lambda \int n_e dl$, where φ is the interferometric phase shift. Using Abel inversion, a multi-chord polarimeter-interferometer has been demonstrated capable to determine the toroidal current profile in tokamak plasmas[3], by computing the electron density and the poloidal magnetic field profiles and then calculating the toroidal current profile via Ampere's law.

Recently, Faraday-effect polarimetry-interferometry utilizing the three-wave technique[4] has advanced with higher resolution in phase[5], space[6] and time[7]. The three-wave technique launches two collinear, counter-rotating circularly-polarized probe beams into the plasma. Faraday rotation is determined by measuring the phase difference between the two probe beams. The line-integrated density is obtained from the averaged phase change of the two probe beams, with respect to a reference beam external to the plasma. By using the three-wave technique, the current profile has been measured with 0.01 MA/m^2 resolution on MST[8] and J-TEXT[9]. To date, pedestal current profile measurements using polarimetry has not been reported. In this paper, we propose a three-wave Faraday-effect polarimeter-interferometer with a sub-centimeter spatial resolution for the DIII-D tokamak to determine the pedestal current profile. While either Abel inversion or equilibrium reconstruction[10] may be used to derive the current profile, the former is investigated herein. The proposed diagnostic will provide not only cross-validation to existing measurements[11], but also new information such as temporal evolution of the pedestal current profile to improve physics understanding. The proposed diagnostic is described in section II. Diagnostic performance is estimated in section III. Uncertainty of the current profile measurement is evaluated in section IV.

[a)]chenje@ucla.edu.

II. DIAGNOSTIC DESCRIPTION

The conceptual setup of the proposed three-wave polarimeter-interferometer is shown in Figure 1. The wavelength is chosen as 316 μm (940 GHz). In the pedestal of typical DIII-D H-mode discharges with 1 MA plasma current, 2 Tesla toroidal magnetic field and 5×10^{19} m^{-3} line-averaged electron density, Faraday rotation angle ranges from 1 to 3 degrees, whereas the coupling to Cotton-Mouton effect[12] is less than 0.001 degree and therefore negligible. The 940 GHz microwave source is commercially available from Virginia Diode Inc. Two collinear right- and left-handed circularly-polarized probe beams pass through the low-field side (LFS) plasma edge vertically (red bar in Figure 2). The probe beams extend radially from R=2.15 to 2.27 m, covering the entire pedestal region (R=2.18-2.23 m; last-closed-flux-surface (LCFS) at R=~2.23m). The radial coverage is achieved by beam expansion using parabolic mirrors and the divergence of the expanded probe beams is negligible (<1 mrad) in the pedestal region. The emergent probe beams from the plasma are combined with a reference beam (not shown in Figure 1) and then directed to a compact, linear detector array. By using the expanded probe beams and the linear detector array, the spatial resolution is limited

Review of Scientific Instruments
ACCEPTED MANUSCRIPT
This is the author's peer reviewed, accepted manuscript. However, the online version of record will be different from this version once it has been copyedited and typeset.
PLEASE CITE THIS ARTICLE AS DOI:10.1063/5.0101550
AIP Publishing

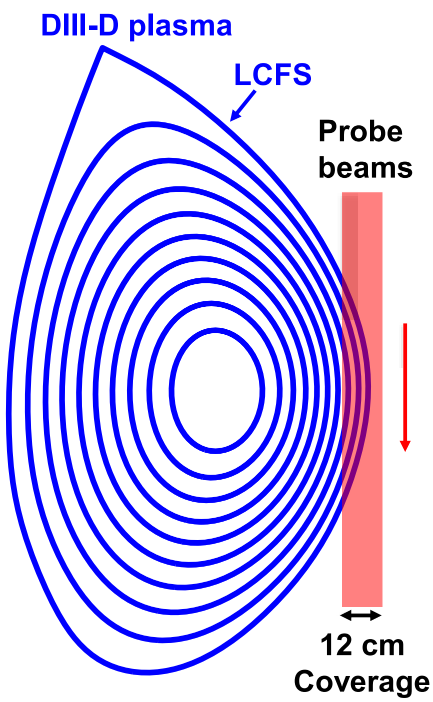

Figure 1 The conceptual setup of the proposed three-wave polarimeter-interferometer for the pedestal current measurement

only by the detector width. Fifteen detectors with 0.8 cm width will be implemented by using commercial 940 GHz planar Schottky diode mixers from Virginia Diode Inc. The time response, set by the frequency separation between the two probe beams and the reference beam, can be up to 10 MHz. For the equilibrium current profile measurement, 1 kHz bandwidth is considered sufficient and assumed in following analysis.

III. ESTIMATE OF DIAGNOSTIC PERFORMANCE

Performance of the proposed diagnostic is estimated by referencing reported performance of existing systems on fusion devices. Specifically, three-wave polarimeter-interferometer systems on MST[13,14], J-TEXT[15], EAST[16,17] and DIII-D[7], which operate at wavelengths (432 to 461 µm) similar to the proposed diagnostic, are considered (Table 1). Performance is characterized by the systematic uncertainty and the root-mean-square (RMS) noise of the polarimeter and the interferometer, respectively. For simplicity, the systematic uncertainty considered here corresponds to the reported dominant uncertainty, although more than one systematic uncertainty may exist.

For polarimetric measurements, the MST and J-TEXT systems, both of which have a single-pass configuration, report non-collinearity[13] as the dominant systematic uncertainty. To minimize this uncertainty, a rotating wedge technique has been developed and a non-collinearity uncertainty below 0.01 degree has been reported on MST[12]. The EAST and DIII-D systems report optical feedback[7,14] as the dominant systematic uncertainty, attributed largely to their double-pass configuration. Mitigation techniques[14] have been reported to reduce the feedback to about 1 degree on EAST and 0.5 to 1 degree on DIII-D, still dominant over the non-collinearity uncertainty. To avoid a large feedback uncertainty, the proposed system will adopt the single-pass configuration (Figure 1). Therefore, it is considered feasible to achieve a systematic polarimetric uncertainty no greater than 0.1 degree, comparable to the MST and J-TEXT systems.

For interferometric measurements, both the J-TEXT[15] and the EAST[17] systems report mechanical vibration as the dominant systematic uncertainty and have adopted various vibration mitigation techniques reducing the mechanical vibration uncertainty to below 2 degrees. In addition, the J-TEXT system uses an in-vacuum reference chord, enabled by radially expanded probe beams and a large window size, to further reduce the mechanical vibration. The proposed DIII-D system will also have expanded probe beams and can implement an in-vessel reference chord if necessary. Therefore, it is considered feasible to achieve a systematic interferometric uncertainty no greater than 2 degrees, comparable to the J-TEXT and EAST systems.

For RMS noise, values shown in Table 1 have been translated from the reported bandwidths to the proposed 1 kHz bandwidth. A reduction of RMS noise is observed over years, i.e. the DIII-D system in 2018[7] shows lower RMS noise than the MST system in 2010[13], likely related to advancement of THz source and detector techniques. Therefore, the proposed system using latest source and detector techniques should be able to achieve RMS polarimetric and interferometric noise no greater than 0.01 and 0.1 degree respectively, similar to the J-TEXT, the EAST and the DIII-D systems. The estimated performance of the proposed system is summarized in the last row of Table 1. It should be emphasized that these estimates have already been achieved in the referenced systems and do not require any further technical improvement.

Table 1 Performances of existing and proposed systems

Device	Systematic uncertainty [degree]		RMS noise at 1kHz bandwidth [degree]	
	Pol.	Int.	Pol.	Int.
MST[13,14]	≤0.01	N/A	~0.03	~0.28
J-TEXT[15]	~0.2	~1	~0.01	~0.14
EAST[16,17]	~1	~2	~0.01	~0.14
DIII-D[7]	0.5-1	N/A	~0.01	~0.03
Proposed	≤0.1	≤2	≤0.01	≤0.1

IV. CURRENT PROFILE UNCERTAINTY

By using synthetic diagnostic calculations and the estimated performance described above, the uncertainty of determining the pedestal current profile is evaluated. A typical DIII-D H-mode plasma (shot #183225 at t=2700 ms) with 1 MA plasma current and $4.5\times10^{19}\mathrm{m}^{-3}$ line-averaged electron density is used for the evaluation. Kinetic equilibrium profiles of the plasma, which include kinetic effects such as the bootstrap current[18], are used to compute

ACCEPTED MANUSCRIPT
Review of Scientific Instruments
This is the author's peer reviewed, accepted manuscript. However, the online version of record will be different from this version once it has been copyedited and typeset.
PLEASE CITE THIS ARTICLE AS DOI:10.1063/5.0101550
AIP Publishing

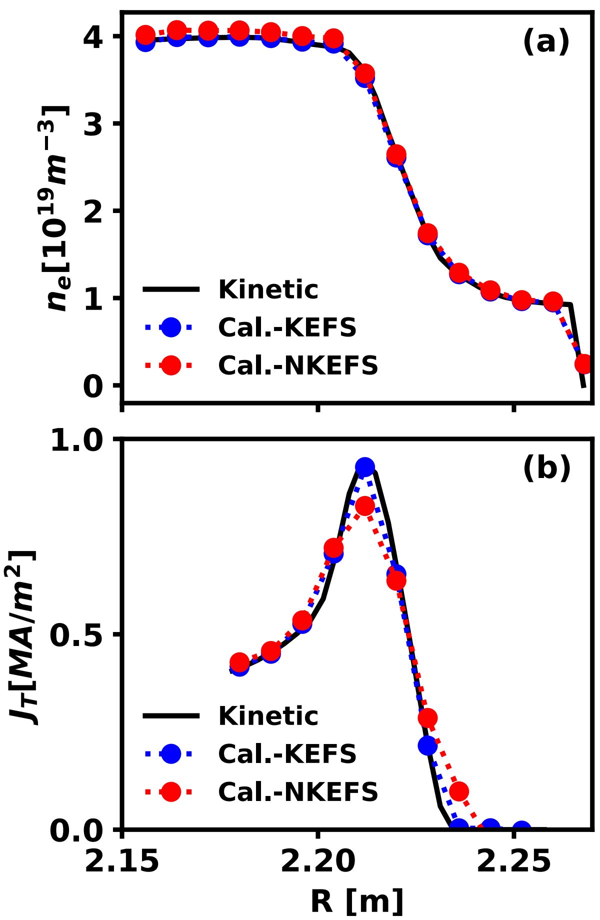

Figure 2 (a) Electron density and (b) Current density: the kinetic equilibrium profiles in black solid lines, the calculated profiles using kinetic equilibrium flux surfaces (KEFS) in blue dash lines and the calculated profiles using non-kinetic equilibiurm flux surfaces (NKEFS) in red dash lines. Solid dots indicate chord locations of the synthesized diagnostic

polarimetric and interferometric signals. Flux surfaces of the kinetic equilibrium is shown in Figure 1 (blue solid lines). The kinetic electron density (n_e) and the toroidal current (J_T) profiles at the LFS mid-plane are shown in Figure 2 (black solid lines). The pedestal region corresponds to R=2.18 to 2.23 m, where a steep n_e gradient and a J_T peak exists. The calculation uses 15 chords with a 0.8 cm spatial resolution and covers from 2.15 m to 2.27 m, unless otherwise noticed. Abel inversion[3] takes the synthesized signals and the flux surfaces as inputs to calculate inverted n_e and poloidal magnetic field (B_p) profiles. Optical refraction effect is less than 1 mrad for the investigated plasma and therefore ignorable – refraction can be corrected in the inversion if not negligible[9]. The toroidal current profile J_T is computed using Ampere's law $J_T = (\nabla \times B_p)/\mu_0$, where μ_0 is the permeability of free space. The J_T uncertainty is defined as the absolute difference between the calculated and kinetic J_T profiles averaged across the pedestal region, that is

$$\epsilon_{J_T} = \overline{|J_{T,calculated} - J_{T,kinetic}|}_{R=2.18-2.23m} \quad (1)$$

In the following, the J_T uncertainty is evaluated by considering various uncertainties from the measurement and the inversion, including quality of flux surfaces (section IV. A), the RMS phase noise (section IV. B), the systematic phase uncertainties (section IV.C) and the spatial resolution and uncertainty (section IV.D).

A. Impact of flux surfaces

The quality of flux surfaces can affect accuracy of Abel inversion. To assess this effect, the J_T uncertainty is evaluated by firstly using the flux surfaces from the kinetic equilibrium. The synthetic signals are calculated without considering any phase noise or systematic uncertainty. The calculated profiles from inversion are then expected to be the same as the kinetic profiles. As shown in Figure 2, the calculated n_e and J_T profiles (blue dashed lines) do have very good agreement with the kinetic profiles (black solid lines). The J_T uncertainty is 0.01 MA/m^2, negligible compared to the peak J_T value (1 MA/m^2). It should be noted that the calculated J_T for edge chords (R<2.17 m and R>2.26 m) tends to be noisy due to the differential J_T calculation of Ampere's law and is not shown in Figure 2(b). The n_e uncertainty, defined in the same manner as the J_T uncertainty (Equation 1), is 2×10^{17}m^{-3} and also negligible. The J_T and n_e uncertainties are likely due to numerical errors in the inversion process and the finite spatial resolution of the synthetic diagnostic. The results show clearly that determining pedestal n_e and J_T profiles accurately from polarimetric and interferometric measurements via Abel inversion is feasible in principle, although the measurements are line-integrated and the 0.8 cm spatial resolution is not much smaller than the total pedestal width (5 cm).

In comparison, the calculated n_e and J_T profiles using flux surfaces from a non-kinetic equilibrium are shown by red dashed lines in Figure 2. The non-kinetic equilibrium is routinely available on DIII-D tokamak and the most readily used source of flux surfaces for Abel inversion. The non-kinetic equilibrium is inherently different from the kinetic equilibrium because no kinetic effects are included. For the investigated plasma, the difference can be seen, for example, from the edge safety factor, which is 5.07 and 4.81 using the kinetic and non-kinetic equilibrium, respectively. The calculated J_T profile using the non-kinetic flux surfaces deviates from but still largely replicates the kinetic J_T profile, such as the peak location and the width. The J_T and n_e uncertainty is 0.04 MA/m^2 and 6×10^{17}m^{-3} respectively, slightly increased compared to the uncertainties using the kinetic equilibrium flux surfaces. The results indicate the quality of flux surfaces has a small impact to the J_T measurement. The non-kinetic flux surfaces are used in the following analysis to simulate experimental conditions.

B. Impact of RMS noise

The RMS noise is simulated by adding random values into the synthesized polarimetric and interferometric signals at each chord, satisfying the normal distribution with a given standard deviation σ. The J_T and n_e uncertainties are ensemble-averaged from fifty independent simulations so that all distributions of the RMS noise are considered as possible. Impact of the RMS noise is evaluated by allowing

ACCEPTED MANUSCRIPT
Review of Scientific Instruments
AIP Publishing
This is the author's peer reviewed, accepted manuscript. However, the online version of record will be different from this version once it has been copyedited and typeset.
PLEASE CITE THIS ARTICLE AS DOI:10.1063/5.0101550

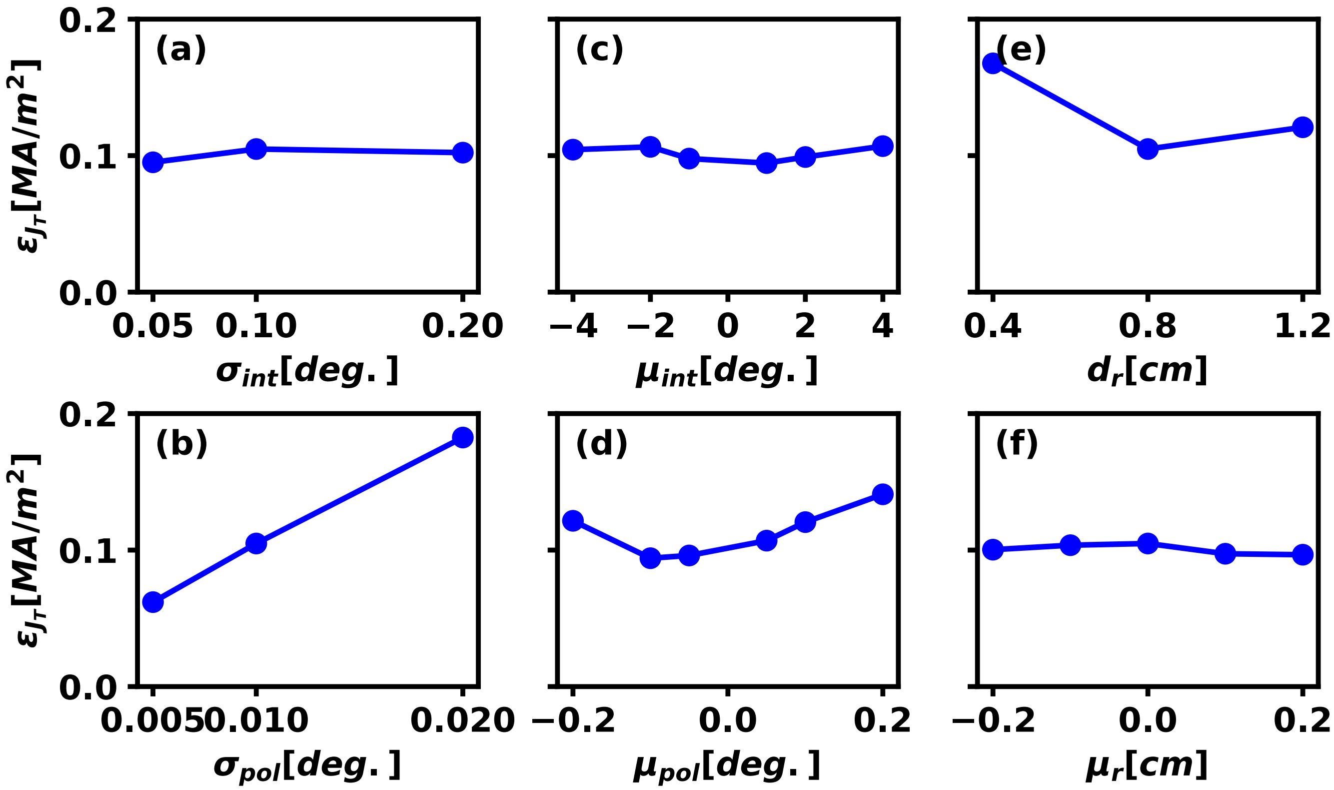

Figure 3 The J_T uncertainty versus (a) the interferometric RMS noise, (b) the polarimetric RMS noise, (c) the interferometric systematic uncertainty, (d) the polarimetric systematic uncertainty, (e)the spatial resolution and (f)the spatial uncertainty

it to vary from 50% to 200% of the estimated values in Table 1. Figure 3(a) presents the J_T uncertainty versus the interferometric RMS noise σ_{int} , with a constant polarimetric RMS noise σ_{pol} at 0.01 degree. The J_T uncertainty is near 0.1 MA/m^2 and exhibits no obvious variation. Similarly, the J_T uncertainty versus σ_{pol} with a constant σ_{int} at 0.1 degree is shown in Figure 3(b). The J_T uncertainty increases rapidly from 0.06 MA/m^2 to 0.18 MA/m^2. The strong J_T uncertainty dependence on σ_{pol} is likely because the random nature of RMS noise has a large impact to the differential J_T calculation. These results indicate minimizing σ_{pol} is essential to achieve an accurate J_T measurement while minimizing σ_{int} is not as critical. The following analysis sets σ_{int} and σ_{pol} to 0.1 and 0.01 degree, respectively, i.e. the estimated values in Table 1, to simulate experimental conditions.

C. Impact of systematic uncertainties

Systematic uncertainties, such as the non-collinearity of probe beams[14] and the optical feedback[16], are difficult to model due to their complicated nature. For simplicity, the systematic uncertainty is simulated by adding a constant value μ to the synthesized polarimetric and interferometric signals at all chords. This is justified for two reasons: 1) some systematic uncertainties, such as the mechanical vibration, tend to be comparable at all chords; 2) a systematic uncertainty, which may introduce random errors at each chord, will have similar effects as the RMS noise evaluated in section IV. B. Therefore, it is of more interest to evaluate impact of comparable errors at all chords in this section. Impact of the systematic uncertainties is evaluated by varying the systematic uncertainties from 50% to 200% of the estimated values in Table 1. In Figure 3(c) and 3(d), the J_T uncertainty versus the systematic interferometric uncertainty μ_{int} and the polarimetric uncertainty μ_{pol} are plotted. The J_T uncertainty shows a negligible impact from the μ_{int} scan, and a modest increase from 0.1 to 0.14 MA/m^2 when μ_{pol} is increased to 0.2 degree. These results indicate suppressing μ_{pol} is more important than suppressing μ_{int}. The scanned range of the systematic uncertainties is an order of magnitude wider than the RMS noise (Figure 3, (a) and (b)), indicating the J_T measurement has a larger tolerance to the systematic uncertainties than the RMS noise. This may be explained by the fact that comparable errors at all chords tend to be cancelled in the differential J_T calculation while random errors are not. Therefore, it is possible that the evaluation in this section might underestimate the J_T uncertainty associated with the systematic uncertainty, if any systematic uncertainty is not comparable or even random across all chords.

D. Impact of spatial resolution and uncertainty

The J_T uncertainty is evaluated using spatial resolution of 0.4, 0.8 and 1.2 cm (Figure 3(e)). Interestingly, the J_T uncertainty is similar (~0.11 MA/m^2) for spatial resolutions at 0.8 and 1.2 cm and increases to 0.17 MA/m^2 for the spatial resolution at 0.4 cm. Again, the results are likely related to the differential J_T calculation. For the same RMS noises level, a smaller spatial resolution generates larger

Review of Scientific Instruments ACCEPTED MANUSCRIPT

This is the author's peer reviewed, accepted manuscript. However, the online version of record will be different from this version once it has been copyedited and typeset.
PLEASE CITE THIS ARTICLE AS DOI:10.1063/5.0101550

AIP Publishing

error in the differential calculation. On the other hand, the 1.2 cm spatial resolution provides fewer spatial points, unfavorable for characterizing a J_T profile with steep gradients. The 0.8 cm spatial resolution appears to be the optimal choice.

Experimentally, the relative position between chords is determined within the detector array and the associated uncertainty can be mechanically determined to within 0.1 mm or less. However, a radial position uncertainty of the entire detector array relative to the vacuum vessel, which is the same for all chords, could occur at a sub-centimeter level. Impact of this radial position uncertainty μ_r ranging from -0.2 to 0.2 cm is evaluated and found negligible, as shown in Figure 3(f).

V. Discussions and Summary

The evaluation in section IV shows that the proposed diagnostic with the estimated performances (Table 1) can determine the pedestal current profile with no greater than 0.12 MA/m^2 uncertainty, or about 10% of the peak J_T value in the investigated plasma pedestal, which is considered useful for physics analysis. Although the polarimetric and interferometric measurements are line-integrated and the 0.8 cm spatial resolution is not much smaller than the pedestal width (5 cm), the J_T profile, such as its peak location and width, can be determined relatively well (Figure 2). The J_T uncertainty is strongly affected by performances of the polarimeter but not the interferometer. It is envisaged that suppressing the polarimetric RMS noise and the polarimetric systematic uncertainty is the key to achieving good pedestal current profile measurements. It should be noted that time averaging of the diagnostic signals can always be used to suppress any random noise or uncertainty, at the expense of the temporal resolution of the measurement.

To summarize, a three-wave polarimeter-interferometer is proposed to determine the H-mode pedestal current profile via Abel inversion in the DIII-D tokamak. The diagnostic would operate at 316 μm and is estimated capable of achieving no greater than 0.01 degree polarimetric RMS noise, no greater than 0.1 degree polarimetric uncertainty and a 0.8 cm spatial resolution. The estimated diagnostic performance is found capable of determining the pedestal current profile with a 0.12 MA/m^2 uncertainty for the investigated H-mode plasma.

This material is based upon work supported by the Department of Energy under Award Numbers DE-SC0019004 and DE-FC02-04ER54698.

Disclaimer: This report was prepared as an account of work sponsored by an agency of the United States Government. Neither the United States Government nor any agency thereof, nor any of their employees, makes any warranty, express or implied, or assumes any legal liability or responsibility for the accuracy, completeness, or usefulness of any information, apparatus, product, or process disclosed, or represents that its use would not infringe privately owned rights. Reference herein to any specific commercial product, process, or service by trade name, trademark, manufacturer, or otherwise does not necessarily constitute or imply its endorsement, recommendation, or favoring by the United States Government or any agency thereof. The views and opinions of authors expressed herein do not necessarily state or reflect those of the United States Government or any agency thereof.

DATA AVAILABILITY

The data that support the findings of this study are available from the corresponding author upon reasonable request.

References

[1] P.B. Snyder, R.J. Groebner, J.W. Hughes, T.H. Osborne, M. Beurskens, A.W. Leonard, H.R. Wilson, and X.Q. Xu, Nucl. Fusion **51**, 103016 (2011).

[2] O. Sauter, C. Angioni, and Y.R. Lin-Liu, Physics of Plasmas **6**, 2834 (1999).

[3] H. Soltwisch, Review of Scientific Instruments **57**, 1939 (1986).

[4] G. Dodel and W. Kunz, Infrared Physics **18**, 773 (1978).

[5] D.L. Brower, W.X. Ding, S.D. Terry, J.K. Anderson, T.M. Biewer, B.E. Chapman, D. Craig, C.B. Forest, S.C. Prager, and J.S. Sarff, Review of Scientific Instruments **74**, 1534 (2003).

[6] D.L. Brower, Y. Jiang, W.X. Ding, S.D. Terry, N.E. Lanier, J.K. Anderson, C.B. Forest, and D. Holly, Review of Scientific Instruments **72**, 1077 (2001).

[7] J. Chen, W.X. Ding, D.L. Brower, D. Finkenthal, and R. Boivin, Review of Scientific Instruments **89**, 10B101 (2018).

[8] D.L. Brower, W.X. Ding, S.D. Terry, J.K. Anderson, T.M. Biewer, B.E. Chapman, D. Craig, C.B. Forest, S.C. Prager, and J.S. Sarff, Phys. Rev. Lett. **88**, 185005 (2002).

[9] J. Chen, G. Zhuang, X. Jian, Q. Li, Y. Liu, L. Gao, and Z.J. Wang, Review of Scientific Instruments **85**, 103501 (2014).

[10] L.L. Lao, H.E.S. John, Q. Peng, J.R. Ferron, E.J. Strait, T.S. Taylor, W.H. Meyer, C. Zhang, and K.I. You, Fusion Science and Technology **48**, 968 (2005).

[11] D.M. Thomas, A.W. Leonard, L.L. Lao, T.H. Osborne, H.W. Mueller, and D.F. Finkenthal, Phys. Rev. Lett. **93**, 065003 (2004).

[12] J. Chen, W.X. Ding, and D.L. Brower, Plasma Phys. Control. Fusion **60**, 085001 (2018).

[13] W.X. Ding, D.L. Brower, W.F. Bergerson, and L. Lin, Review of Scientific Instruments **81**, 10D508 (2010).

[14] L. Lin, W.X. Ding, and D.L. Brower, Review of Scientific Instruments **83**, 10E320 (2012).

[15] J. Chen, G. Zhuang, Q. Li, Y. Liu, L. Gao, Y.N. Zhou, X. Jian, C.Y. Xiong, Z.J. Wang, D.L. Brower, and W.X. Ding, Review of Scientific Instruments **85**, 11D303 (2014).

[16] Z.Y. Zou, H.Q. Liu, W.X. Ding, J. Chen, D.L. Brower, H. Lian, S.X. Wang, W.M. Li, Y. Yao, L. Zeng, and Y.X. Jie, Review of Scientific Instruments **89**, 013510 (2018).

[17] H.Q. Liu, J.P. Qian, Y.X. Jie, W.X. Ding, D.L. Brower, Z.Y. Zou, W.M. Li, H. Lian, S.X. Wang, Y. Yang, L. Zeng, T. Lan, Y. Yao, L.Q. Hu, X.D. Zhang, and B.N. Wan, Review of Scientific Instruments **87**, 11D903 (2016).

[18] T.H. Osborne, G.L. Jackson, Z. Yan, R. Maingi, D.K. Mansfield, B.A. Grierson, C.P. Chrobak, A.G. McLean, S.L. Allen, D.J. Battaglia, A.R. Briesemeister, M.E. Fenstermacher, G.R. McKee, and P.B.S. and, Nucl. Fusion **55**, 063018 (2015).

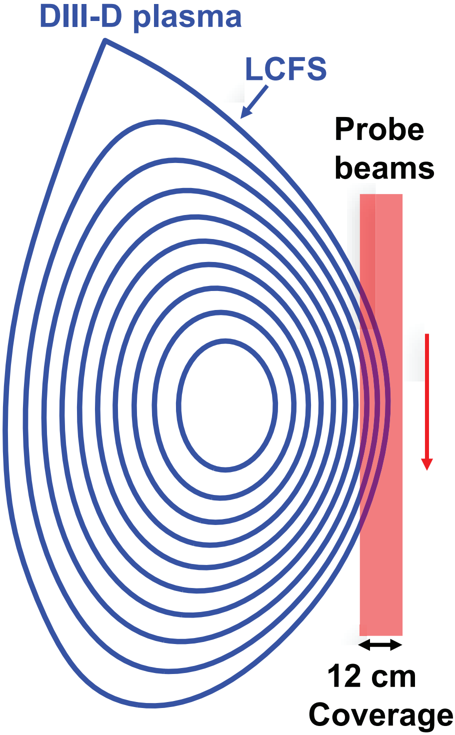
DIII-D plasma
LCFS
Probe
beams
12 cm
Coverage

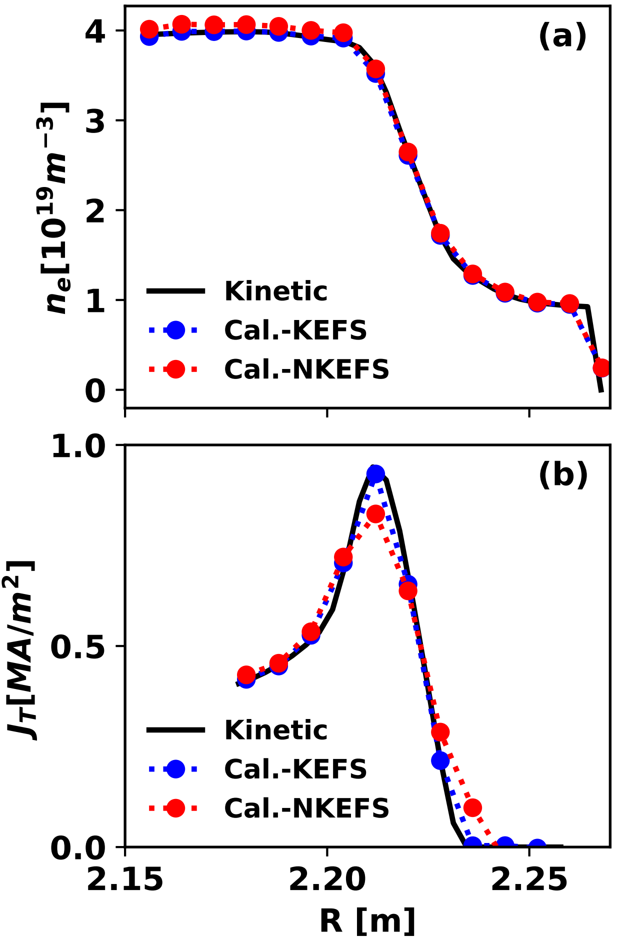

(a)
$n_e[10^{19}m^{-3}]$
4
3
2
1
0
Kinetic
Cal.-KEFS
Cal.-NKEFS
(b)
$J_T[MA/m^2]$
1.0
0.5
0.0
Kinetic
Cal.-KEFS
Cal.-NKEFS
2.15
2.20
2.25
R [m]

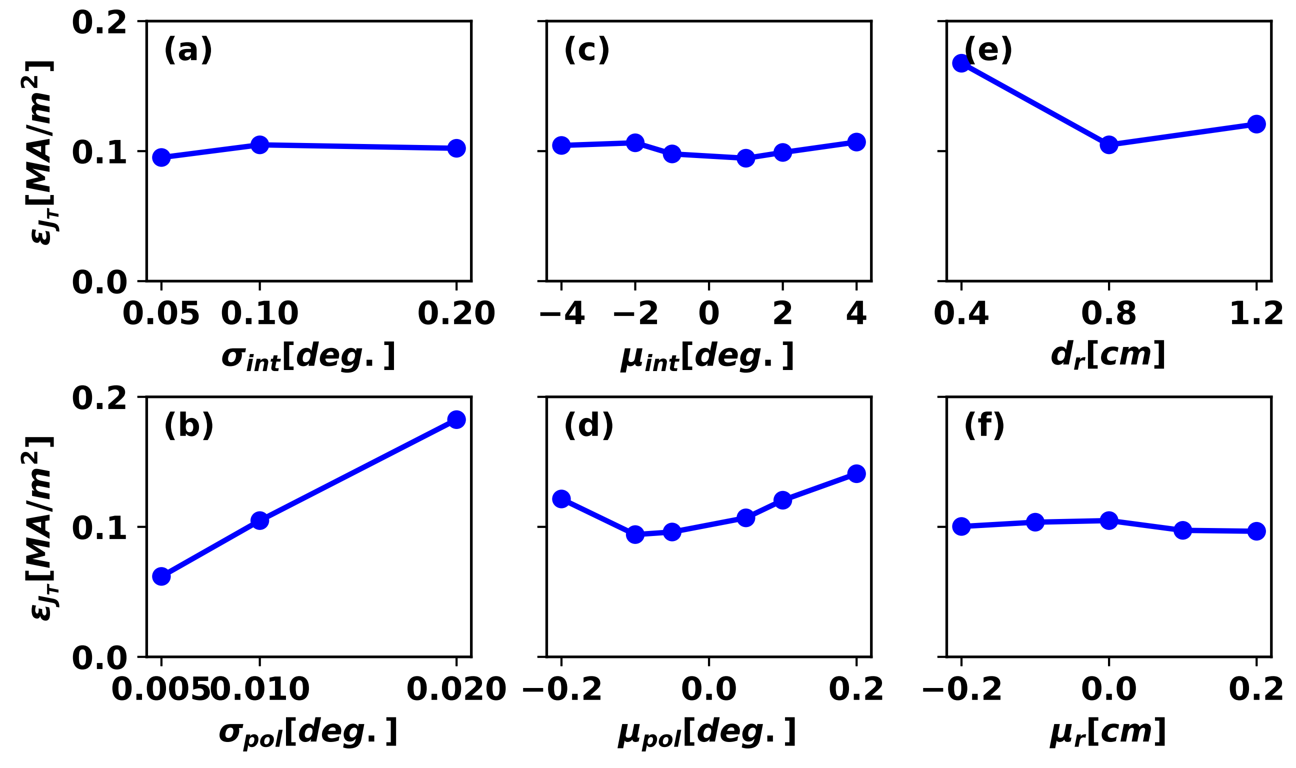

(a)
(b)
(c)
(d)
(e)
(f)
$\varepsilon_{J_T}[MA/m^2]$
$\sigma_{int}[deg.]$
$\mu_{int}[deg.]$
$d_r[cm]$
$\sigma_{pol}[deg.]$
$\mu_{pol}[deg.]$
$\mu_r[cm]$
0.0
0.1
0.2
0.05
0.10
0.20
−4
−2
0
2
4
0.4
0.8
1.2
0.005
0.010
0.020
−0.2
0.0
0.2